

# $\Lambda$ -hyperon interaction with nucleons

M. Ikram<sup>1</sup>, S. K. Singh<sup>2</sup>, S. K. Biswal<sup>2</sup>, M. Bhuyan<sup>2</sup>, and S. K. Patra<sup>2</sup>

<sup>1</sup>*Department of Physics, Aligarh Muslim University, Aligarh - 202002, India and*

<sup>2</sup>*Institute of Physics, Sachivalaya Marg, Bhubaneswar - 751005, India.*

(Dated: January 16, 2014)

We study the interaction of  $\Lambda$ -hyperon with proton and neutron inside a nucleus within the framework of relativistic mean field formalism. The single particle energy levels for some of the specific proton and neutron orbits are analyzed with the addition of  $\Lambda$ -successively. We found that the interaction of  $\Lambda$  with neutron is more stronger than proton.

PACS numbers: 21.10.-k, 21.10.Dr, 21.80.+a

Hypernucleus provides an opportunity to enter into the strangeness world. After introducing the strangeness degree of freedom to bound nuclear system, the multi-baryonic system avails  $\Lambda$ -nucleon ( $\Lambda N$ ) interaction in addition to nucleon-nucleon (NN) interaction. However,  $\Lambda N$  interaction is weaker than NN but it is imperative as well as important to describe the strange system. Many of the theoretical calculations have been made to give the importance of  $\Lambda N$  interaction and to facilitate the path toward multi-strange systems [1–5].

The information about the hyperon-nucleon interaction especially  $\Lambda p$  and  $\Lambda n$  can be extracted from the hypernuclei. Due to zero isospin of  $\Lambda$ -hyperon, the one pion exchange is prohibited in  $\Lambda N$  interaction. Which means the  $\Lambda N$  interaction is governed by two pion exchange. In this way,  $\Lambda N - \Sigma N$  coupling plays a significant role to drive the  $\Lambda N$  interaction. The most interested mirror hypernuclei are  ${}^4_{\Lambda}\text{H}$  and  ${}^4_{\Lambda}\text{He}$  which reflect the difference in strength of  $\Lambda p$  and  $\Lambda n$  interactions. The  $\Lambda N$  interaction occurs via  $\Lambda N - \Sigma N$  coupling where,  $\Lambda p$  couples to  $\Sigma^+ n$  and  $\Lambda n$  is coupled with  $\Sigma^- p$  [6]. Therefore,  $\Sigma N$  plays a role as an intermediate state to access the  $\Lambda N$  interaction. On the basis of this coupling, it is expected that the mass difference of  $\Sigma^+ - \Sigma^-$  is responsible to make a difference in the strength of  $\Lambda p$  and  $\Lambda n$  interactions as discussed in Refs. [2, 6, 7]. The difference in strength of these interactions is a direct consequence of charge symmetry breaking which is observed in mirror hypernuclei [2, 6, 7]. It is well understood that any kinds of change take place in the interaction is directly reflected in nuclear potential as well as single-particle energy. Thus, it is very much interesting to analyze the single-particle energy or potential to study the net effect on interaction, either with the addition of  $\Lambda$ -hyperon or any other effects. In this work, we study the single-particle energy as well as potentials of some medium and superheavy hypernuclei to demonstrate this mechanism by employing the relativistic mean field (RMF) formalism.

Recently, the RMF theory is quite successful for studying the finite and infinite nuclear systems. Quite successful to study the equation of state (EOS) for normal as well as high dense neutron matter. Since neutron star is a compact object with nuclear density  $\rho = (8 - 10)\rho_0$ , where  $\rho_0$  is the nuclear matter density at saturation,

so there must be the possibility of formation of strange baryon. In this context, addition of strangeness degree of freedom to RMF formalism is obvious for the suitable expansion of the model and this type of attempts have already been made [4, 8–17].

The relativistic mean field Lagrangian density for single- $\Lambda$  hypernuclei has been given in Refs. [8, 9, 11–13, 15, 17]. To study the multi-strange system in quantitative way, the additional strange scalar ( $\sigma^*$ ) and vector ( $\phi$ ) mesons have been included which simulate the  $\Lambda\Lambda$  interaction [4, 10, 14, 16]. Now, the total Lagrangian density can be written as

$$\mathcal{L} = \mathcal{L}_N + \mathcal{L}_\Lambda + \mathcal{L}_{\Lambda\Lambda}, \quad (1)$$

$$\begin{aligned} \mathcal{L}_N &= \bar{\psi}_i \{ i\gamma^\mu \partial_\mu - M \} \psi_i + \frac{1}{2} (\partial^\mu \sigma \partial_\mu \sigma - m_\sigma^2 \sigma^2) - \frac{1}{3} g_2 \sigma^3 \\ &\quad - \frac{1}{4} g_3 \sigma^4 - g_s \bar{\psi}_i \psi_i \sigma - \frac{1}{4} \Omega^{\mu\nu} \Omega_{\mu\nu} + \frac{1}{2} m_\omega^2 \omega^\mu \omega_\mu \\ &\quad - g_\omega \bar{\psi}_i \gamma^\mu \psi_i \omega_\mu - \frac{1}{4} B^{\mu\nu} B_{\mu\nu} + \frac{1}{2} m_\rho^2 \rho^\mu \rho_\mu - \frac{1}{4} F^{\mu\nu} F_{\mu\nu} \\ &\quad - g_\rho \bar{\psi}_i \gamma^\mu \vec{\tau} \psi_i \vec{\rho}_\mu - e \bar{\psi}_i \gamma^\mu \frac{(1 - \tau_{3i})}{2} \psi_i A_\mu, \\ \mathcal{L}_\Lambda &= \bar{\psi}_\Lambda \{ i\gamma^\mu \partial_\mu - m_\Lambda \} \psi_\Lambda - g_{\sigma\Lambda} \bar{\psi}_\Lambda \psi_\Lambda \sigma - g_{\omega\Lambda} \bar{\psi}_\Lambda \gamma^\mu \psi_\Lambda \omega_\mu, \\ \mathcal{L}_{\Lambda\Lambda} &= \frac{1}{2} (\partial^\mu \sigma^* \partial_\mu \sigma^* - m_{\sigma^*}^2 \sigma^{*2}) - \frac{1}{4} S^{\mu\nu} S_{\mu\nu} + \frac{1}{2} m_\phi^2 \phi^\mu \phi_\mu \\ &\quad - g_{\sigma^*\Lambda} \bar{\psi}_\Lambda \psi_\Lambda \sigma^* - g_{\phi\Lambda} \bar{\psi}_\Lambda \gamma^\mu \psi_\Lambda \phi_\mu, \end{aligned} \quad (2)$$

where  $\psi$  and  $\psi_\Lambda$  denote the Dirac spinors for nucleon and  $\Lambda$ -hyperon, whose masses are  $M$  and  $m_\Lambda$  respectively. Because of zero isospin, the  $\Lambda$ -hyperon does not couple to  $\rho$ -mesons. The quantities  $m_\sigma$ ,  $m_\omega$ ,  $m_\rho$ ,  $m_{\sigma^*}$ ,  $m_\phi$  are the masses of included mesons and  $g_s$ ,  $g_\omega$ ,  $g_\rho$ ,  $g_{\sigma\Lambda}$ ,  $g_{\omega\Lambda}$ ,  $g_{\sigma^*\Lambda}$ ,  $g_{\phi\Lambda}$  are their coupling constants. The nonlinear self-interaction coupling of  $\sigma$  mesons is denoted by  $g_2$  and  $g_3$ . The total energy of the system is given by  $E_{total} = E_{part}(N, \Lambda) + E_\sigma + E_\omega + E_\rho + E_{\sigma^*} + E_\phi + E_c + E_{pair} + E_{cm.}$ , where  $E_{part}(N, \Lambda)$  is the sum of the single particle energies of the nucleons (N) and hyperon ( $\Lambda$ ). The energies parts  $E_\sigma$ ,  $E_\omega$ ,  $E_\rho$ ,  $E_{\sigma^*}$ ,  $E_\phi$ ,  $E_c$ ,  $E_{pair}$  and  $E_{cm}$  are the contributions of meson fields, Coulomb field, pairing energy and the center-of-mass energy, respectively. For present study, we use the NL3\* parameter set throughout the calculations [18]. To find the numerical values

of used  $\Lambda$ -meson coupling constants, we adopt the relative coupling for  $\sigma$ ,  $\omega$ ,  $\sigma^*$  and  $\phi$  fields. The ratio of meson-hyperon coupling to meson-nucleon coupling is defined as  $R_\sigma = g_{\sigma\Lambda}/g_\sigma$  and  $R_\omega = g_{\omega\Lambda}/g_\omega$ ,  $R_{\sigma^*} = g_{\sigma^*\Lambda}/g_{\sigma^*}$  and  $R_\phi = g_{\phi\Lambda}/g_\phi$ . The relative coupling values are used as  $R_\omega = 2/3$ ,  $R_\phi = -\sqrt{2}/3$ ,  $R_\sigma = 0.621$  and  $R_{\sigma^*} = 0.69$  [4, 11, 19, 20]. In present calculations, we use the constant gap BCS approximation to include the pairing interaction and the centre of mass correction is included by  $E_{cm} = -(3/4)41A^{-1/3}$ .

The addition of  $\Lambda$ -hyperon to normal nuclei enhances the binding and shrinks the core of the system. This happens because of glue like behaviour of  $\Lambda$ -hyperon. These observations are shown in Table 1, where the total binding energy (BE) of hypernuclei are larger than their normal counter parts and a reduction in total radius ( $r_{rms}$ ) of hypernuclei is also observed. For example, the total radius of  $^{48}\text{Ca}$  is 3.496 fm, which is reduced to 3.454 fm by addition of single  $\Lambda$  into  $^{48}\text{Ca}$  nucleus. The increasing value of single- $\Lambda$  binding energy ( $B_\Lambda$ ) for  $s$ -state from medium to superheavy hypernuclei confirming the potential depth of lambda particle in nuclear matter which would be -28 MeV [4, 22].

The lambda hyperons are introduced into the nucleus to see the effects of substituted hyperons on single particle energies of neutron as well as proton. We choose the system in such a way to cover the range from medium to superheavy hypernuclei, for example,  $^{48}_{n\Lambda}\text{Ca}$ ,  $^{208}_{n\Lambda}\text{Pb}$  and  $^{298}_{n\Lambda}114$ . To study the single particle energy, we choose some specific energy levels (first occupied and other higher orbital) for both neutron as well as proton. Initially, in normal nuclei the higher orbitals of proton and neutron are fully occupied but due to successive addition of  $\Lambda$ -hyperons with replacing neutrons the upper neutron orbitals become unfilled however proton orbitals are still occupied. In this way, we analyze the energy space for first filled and other higher levels with successive addition of  $\Lambda$ -hyperons. In  $^{48}_{n\Lambda}\text{Ca}$ , we study the behaviour of proton ( $1s_{1/2}$ ,  $1d_{3/2}$ ) and neutron ( $1s_{1/2}$ ,  $1f_{7/2}$ ) energy levels in the respect of substituted  $\Lambda$ 's. It is evident from Fig. 1(a, b, c) that the neutron levels go dipper with increasing number of substituted  $\Lambda$ -hyperons. The behaviour of first occupied proton level looks to be in same trend as neutron but feels small attraction comparable to neutron. This observation reflects that the hyperon interact more strongly with neutron in comparison to proton. However, the nature of both the interactions is attractive and the present outcome confirms that  $\Lambda n$  interaction is more stronger than  $\Lambda p$ . Again it is found that, the first occupied orbital of neutron is more effective by addition of  $\Lambda$ 's compared to higher orbitals. For example,  $1s_{1/2}(n)$  orbital feels more attraction in comparison to  $1f_{7/2}(n)$  levels in  $^{48}_{n\Lambda}\text{Ca}$  hypernuclei. This may be expected because of  $\Lambda$ -hyperon resides at the center of the nucleus for most of the time and attracts the surrounding nucleons towards the centre. On the other hand, the higher proton and neutron levels are in opposite trend to each other. In  $^{48}_{n\Lambda}\text{Ca}$  hypernu-

clei, the neutron level ( $1f_{7/2}(n)$ ) feels a small attraction with the addition of successive  $\Lambda$ 's while the proton level ( $1d_{3/2}(p)$ ) seems in opposite trend. This may be because of the Coulomb repulsion. The injected  $\Lambda$ -hyperons reduce the isospin of the whole system and as a result the Coulomb interaction becomes more effective. This mechanism can be explained by higher proton orbital, where it goes toward less bound nature, for example,  $1d_{3/2}(p)$  level in  $^{48}_{n\Lambda}\text{Ca}$ ,  $1h_{11/2}(p)$  level in  $^{208}_{n\Lambda}\text{Pb}$  and  $1i_{13/2}(p)$  level in  $^{298}_{n\Lambda}114$  as shown in Fig. 1(a, b, c). It is also to be noted that the system with strangeness feels to be more bound with the addition of  $\Lambda$ -hyperon successively, and single particle energy levels goes dipper and dipper up to a certain number of hyperons. Beyond this limit the nature of hypernuclear system becomes reversed and would be collapsed as referred as key point in Ref. [10]. This behaviour can be noticed in  $^{48}_{n\Lambda}\text{Ca}$ , where after the addition of 14  $\Lambda$ 's, the neutron and proton potentials are reduced. The same behavior of single particle energy levels is observed not only for  $^{208}_{n\Lambda}\text{Pb}$  but  $^{298}_{n\Lambda}114$  superheavy hypernucleus also as shown in Fig. 1(a, b, c).

The neutron ( $V_N$ ) and lambda ( $V_\Lambda$ ) mean potentials are plotted for the considered hypernuclei in Fig. 1(d, e, f). From this figure, it is reveal that how does the potential shape and depth are affected by successive addition of  $\Lambda$ -hyperons to the core of the nuclei. The behaviour of the potential is plotted only for some number of hyperons. For example, the neutron and lambda mean potentials are given for  $\Lambda = 1, 5, 8$  and 20 for  $^{48}_{n\Lambda}\text{Ca}$ . In the same way for superheavy hypernuclei,  $^{298}_{n\Lambda}114$ , the potentials are shown for  $\Lambda = 1, 20, 40, 60$  and 80. It is shown in Fig. 1d, that the  $V_N$  gets the depth around -85 MeV with addition of one  $\Lambda$  to  $^{48}\text{Ca}$  nucleus and it goes dipper with the addition of more  $\Lambda$ 's. Look into the  $^{208}_{n\Lambda}\text{Pb}$ , both the potential depth ( $V_N$  and  $V_\Lambda$ ) goes dipper with inclusion of 40  $\Lambda$ 's but revert on addition of 60  $\Lambda$ 's. The reason is simple because there is some limitation of numbers of hyperons for a particular system to make the maximum binding. The potentials ( $V_N$  and  $V_\Lambda$ ) are distorted with the addition of 20  $\Lambda$ 's to the core of  $^{48}\text{Ca}$  nucleus. It is clearly seen that the depth and shape of lambda mean potential is completely affected with increasing the  $\Lambda$ -interactions with nucleons.

The present study is fully devoted to demonstrate the difference in strength of  $\Lambda$ -nucleon interactions in multi-baryonic system. The results show that the  $\Lambda n$  interaction is more stronger than  $\Lambda p$  which is in agreement with scattering data. We also observe the affects on  $V_N$  and  $V_\Lambda$  mean potentials by introducing the  $\Lambda$ -hyperons successively. In our study we find that the binding of nuclear system is increasing with increasing the injected hyperons but up to a certain numbers. The injection of all other hyperons in presence of  $\Lambda$  would provide an opportunity to study the high dense system where cluster of baryon octet or pure hyperonic matter may exist. This type of study will be helpful to simulate the structure of astrophysical objects like, neutron or hyperon stars. Work is in progress in this direction.

TABLE I: The calculated total and per particle binding energy for single- $\Lambda$  hypernuclei and their normal counter parts are listed here. The single- $\Lambda$  binding energy for s- and p-state of considered hypernuclei are also mentioned and compared with available exp. values which are given in parentheses [21]. The radii are also displayed. Energies are given in MeV and radii are in fm.

	BE	$B_{\Lambda}^s$	$B_{\Lambda}^p$	$r_{ch}$	$r_{rms}$	$r_n$	$r_{\Lambda}$
$^{48}\text{Ca}$	414.2			3.444	3.496	3.591	
$^{48}_{\Lambda}\text{Ca}$	428.2	21.7	13.4	3.435	3.454	3.554	2.708
$^{208}\text{Pb}$	1639.3			5.499	5.624	5.736	
$^{208}_{\Lambda}\text{Pb}$	1660.1	26.9(26.3 $\pm$ 0.8)	23.0(21.3 $\pm$ 0.7)	5.490	5.602	5.718	4.011
$^{298}_{114}$	2119.3			6.248	6.397	6.513	
$^{298}_{\Lambda}114$	2168.6	27.2	24.1	6.241	6.378	6.497	3.209

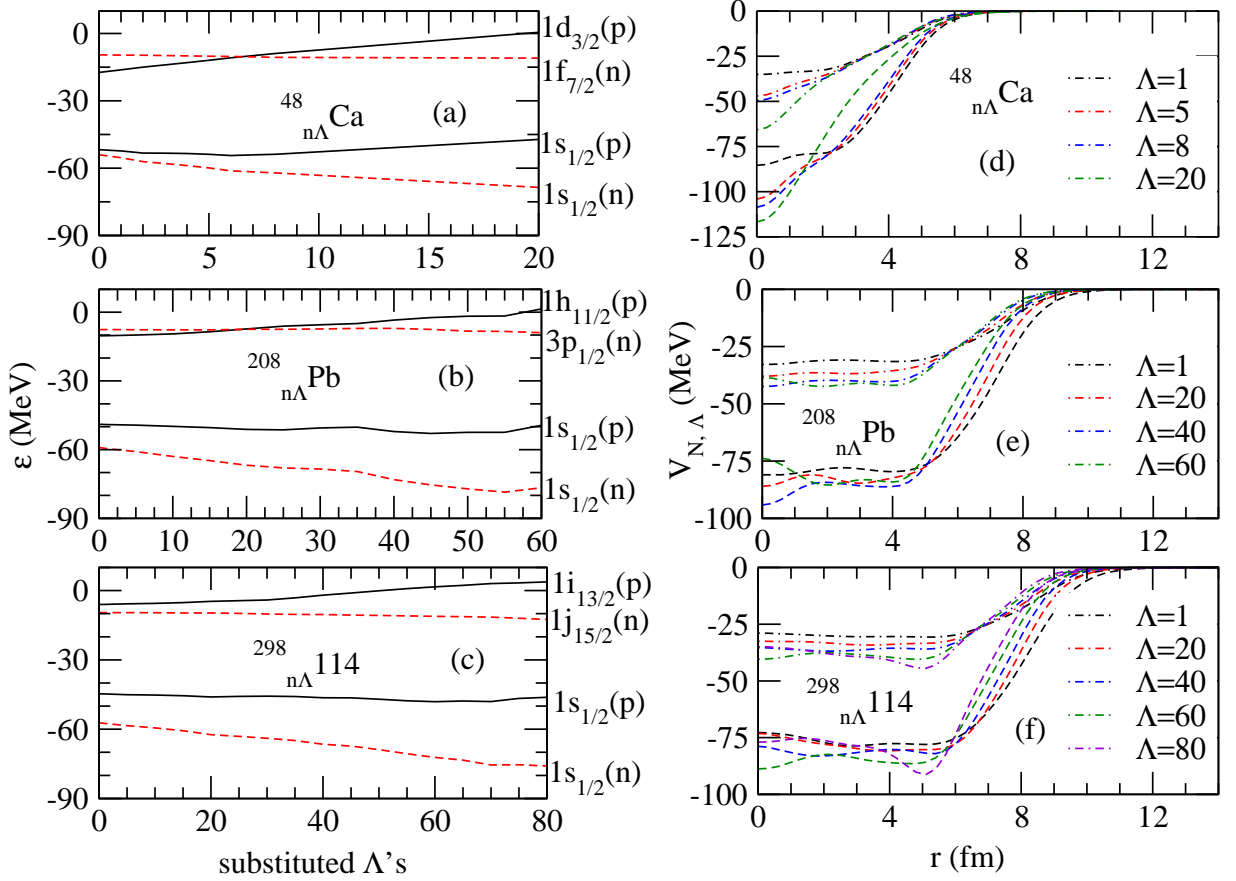


FIG. 1: (color online) The first occupied and higher orbits of neutron and proton are shown for  $^{48}_{n\Lambda}\text{Ca}$ ,  $^{208}_{n\Lambda}\text{Pb}$  and  $^{298}_{n\Lambda}114$  hypernuclei as a function of substituted  $\Lambda$ 's with replacing neutrons on left portion of figure where, the dashed lines in red color represent the neutron levels while the proton levels are represented by solid black lines. The neutron ( $V_N = V_{\sigma} + V_{\omega} + V_{\rho}$ ) and lambda ( $V_{\Lambda} = V_{\sigma\Lambda} + V_{\omega\Lambda}$ ) mean potentials are shown for considered hypernuclei in right portion of the figure. The dashed and dash dotted lines with different colors represent the neutron and lambda mean potential, respectively.

One of the author (MI) wishes to acknowledge the hospitality provided by Institute of Physics, Bhubaneswar

during the work.

- 
- [1] A. R. Bodmer and S. Sampanthar, Nucl. Phys. **31**, 251 (1962).
  - [2] B. F. Gibson, Nucl. Phys. A **479**, 115c (1988).
  - [3] B. F. Gibson, I. R. Afnan, J. A. Carlson and D. R. Lehman, Prog. Theo. Phys. Suppl. **117**, 339 (1994).
  - [4] J. Schaffner, C. B. Dover, A. Gal, C. Greiner, D. J. Millener and H. Stöcker, Ann. Phys. (N.Y.) **235**, 35 (1994).
  - [5] B. F. Gibson and I. R. Afnan, Nucl. Phys. A **914**, 179 (2013).
  - [6] B. F. Gibson and E. V. Hungerford III, Phys. Rep. **257**, 349 (1995).
  - [7] R. H. Dalitz and F. V. Hippel, Phys. Lett. **10**, 153 (1964).
  - [8] M. Rufa, J. Schaffner, J. Maruhn, H. Stöcker, W. Greiner and P. -G. Reinhard, Phys. Rev. C **42**, 2469 (1990).
  - [9] N. K. Glendenning, D. Von-Eiff, M. Haft, H. Lenske and M. K. Weigel, Phys. Rev. C **48**, 889 (1993).
  - [10] J. Schaffner, C. B. Dover, A. Gal, C. Greiner and H. Stöcker, Phys. Rev. Lett. **71**, 1328 (1993).
  - [11] J. Mares and B. K. Jennings, Phys. Rev. C **49**, 2472 (1994).
  - [12] Y. Sugahara and H. Toki, Prog. Theor. Phys. **92**, 803 (1994).
  - [13] D. Vretenar, W. Poßchl, G. A. Lalazissis and P. Ring, Phys. Rev. C **57**, R1060 (1998).
  - [14] J. Schaffner, M. Hanauske, H. Stöcker and W. Greiner, Phys. Rev. Lett. **89**, 171101 (2002).
  - [15] H. -F. Lü, J. Meng, S. Q. Zhang and S. G. Zhou, Eur. Phys. J. A. **17**, 19 (2003).
  - [16] H. Shen, F. Yang and H. Toki, Prog. Theor. Phys. **115**, 325 (2006).
  - [17] M. T. Win and K. Hagino, Phys. Rev. C **78**, 054311 (2008).
  - [18] G. A. Lalazissis, S. Karatzikos, R. Fossion, D. Pena Arteaga, A. V. Afanasjev and P. Ring, Phys. Lett. B **671**, 36 (2009).
  - [19] C. B. Dover and A. Gal, Prog. Part. Nucl. Phys. **12**, 171 (1984).
  - [20] C. M. Keil, F. Hoffmann and H. Lenske, Phys. Rev. C **61**, 064309 (2000).
  - [21] O. Hashimoto, H. Tamura, Prog. Part. Nucl. Phys. **57**, 564 (2006).
  - [22] D. J. Millener, C. B. Dover and A. Gal, Phys. Rev. C **38**, 2700 (1988).